



Effect of Liquid Phase and Vaporization on the Formation of Microstructure of Pr Doped ZnO Varistor

NAOKI WAKIYA¹, SUNG-YONG CHUN¹, CHAE HYUN LEE², OSAMU SAKURAI¹,
KAZUO SHINOZAKI¹ & NOBUYASU MIZUTANI¹

¹*Department of Metallurgy and Ceramic Science, Tokyo Institute of Technology, 2-12-1, Ookayama, Meguro-ku, Tokyo 152, Japan*

²*Division of Advanced Materials Engineering, Pai Chai University, 439-6, Doma-dong, Seo-gu, Taejon, 302-735, Korea*

Submitted November 17, 1997; Revised May 28, 1998; Accepted May 29, 1998

Abstract. Our previous works and our recent data were summarized to discuss the effect of liquid phase formation and vaporization of the components on the densification, grain growth and change of the microstructure of Pr doped ZnO ceramics in air. In the ZnO-Pr₂O₃ binary system, eutectic liquid forms at $1382 \pm 5^\circ\text{C}$ and significant vaporization of the components occurred above the eutectic temperature. Below eutectic temperature (1350°C), only 0.1 mol % of Pr doping into ZnO brought about the grain growth of ZnO, however further addition of Pr brought about the suppression of the grain growth. Comparing the grain size distribution at the surface and inside part of Pr doped ZnO ceramics, it was clarified that wider grain size distribution was observed at the surface than inside part. At the temperature just below the eutectic (1370°C), abnormal grain growth was also observed. Depth profile of Pr content indicated that no concentration gradient was observed below eutectic temperature (1350°C), however above eutectic temperature (1500°C), condensation of Pr was observed at the surface. Grain growth rate as well as weight loss rate were drastically increased between 1350 and 1370°C , which suggested that formation of liquid phase accelerate the grain growth rate and weight loss rate. Consequently the microstructure of Pr doped ZnO ceramics was formed by both effects on the formation of liquid phase and on the vaporization of the components.

Keywords: ZnO varistor, liquid phase, vaporization, microstructure, Praseodymium oxide, Pr₂O₃

1. Introduction

Since the discovery of ZnO base varistor of Bi doped system [1] and Pr doped system [2], so many works has been done till now. It is well known that the varistor characteristics were generated at the grain boundary of ZnO ceramics [3]. Therefore it is very important to clarify the formation mechanism of microstructure especially, grain boundary in ZnO varistor. A variety of varistor-forming oxides such as Bi₂O₃, Pr₆O₁₁, BaO and La₂O₃ with large ionic radii have been used in the past. These dopants segregate at the triple point and grain boundary of ZnO and form intergranular phase.

For Bi doped ZnO, the formation of eutectic liquid phase was observed at 740°C and phase diagram was

reported [4]. On the sintering, the dissolution of ZnO into the Bi-rich intergranular liquid occurred above liquid phase forming temperature. On the slow cooling, the liquid phase form flat interfaces having crystallographic orientation relationship with the basal plane of ZnO grains [5].

For Pr doped ZnO, the formation of liquid phase was proposed by the inflection point in the Arrhenius-type plot of average grain size versus temperature at 1280°C [6]. By applying this method for several composition, the change of liquid-phase-formation temperature with the composition was reported [7].

In our previous work, the effect of several experimental conditions on the formation of the microstructure has been discussed in N₂ and O₂ [8, 9], however, little has been discussed in air. Moreover in

our previous work, the phase diagram of Pr_2O_3 -ZnO system shown in Fig. 1 was established in air using DTA and physical view observations [10]. Figure 1 shows that the formation of eutectic liquid phase was observed at $1382 \pm 5^\circ\text{C}$. In this paper, the summary of our previous works and our recent data were also added to clarify the formation of the microstructure of Pr doped ZnO ceramics, especially, in air.

2. Experimental

ZnO (99.9%, High Purity Chemicals, Japan) and $\text{PrO}_{1.833}$ (Pr_6O_{11}) (99.9%, High Purity Chemicals., Japan) were used as starting materials. Powders having $x\text{PrO}_{1.833} - (1-x)\text{ZnO}$ composition were mixed with ethanol using a plastic jar and ZrO_2 balls for 24 h and dried using a rotary evaporator. The powders were pressed into pellets using a dies of $10\text{ mm}\phi$ in diameter at 100 MPa. The pellets were heated up to prescribed temperature with heating rate of $5.5^\circ\text{C}/\text{min}$. At the prescribed temperature, the samples were sintered for 2 h then they were pulled out quickly from the furnace into room temperature.

The composition of the samples was analyzed using Inductively Coupled Plasma-Atomic Emission Spectrometry (SPS-1500VR, Seiko Instruments, Japan). The composition of whole pellets were also measured. The depth profile of the composition was measured by grinding the pellet step by step from the surface into the bulk and the grounded powder was dissolved in the dilute nitric acid. To avoid the effect

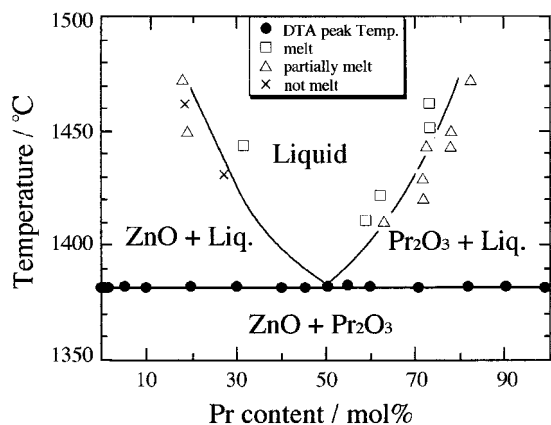


Fig. 1. Experimentally determined ZnO solidus and liquidus boundary for the ZnO- Pr_2O_3 system [10].

of the concentration gradient at the side, the side part of the pellet was removed about $300\ \mu\text{m}$ depth from the surface.

Identification of the resultant phases and lattice parameter measurement were performed by X-ray diffractometer (PW-1700 system, Philips, Netherlands). Si was used as an internal standard and the lattice parameters were determined using the least-squares program RLC-3 [11]. Scanning electron microscope (JSM-T200, Jeol, Japan) was used for the microstructure observation. To obtain average grain size and grain size distribution, linear intercept method [12] was employed. Since Pr_6O_{11} is reduced to Pr_2O_3 above 1200°C [13], the formula " Pr_2O_3 " is used as the expression of praseodymium oxide in the following.

3. Results and Discussion

3.1. Densification and Grain Growth Behavior Below Eutectic Temperature

Figure 2 shows changes of the lattice parameters of (a) ZnO and (b) Pr_2O_3 with Pr content. The lattice parameters were measured for the sample heated at 1400°C for 2 h and quenched into liquid nitrogen. These figures indicate that no noticeable changes of lattice parameters were detected within experimental errors. In this work, the lattice parameters were also measured for the sample heated at 1350°C for 2 h followed by quenching into air. Consequently it was found that the lattice parameters of ZnO were not changed at all by the Pr content, either. These facts suggest that ZnO and Pr_2O_3 do not form the solid solution each other or the solubility of Pr into ZnO and Zn into Pr_2O_3 are very little at both below and above the eutectic temperature.

Figure 3 shows the relationship between the relative density and Pr content after sintered at 1350°C for 2 h. The relative density was increased up to 97% by the addition of small amount of Pr. For rare-earth (Sm, Eu, Y and Er) doped ZnO, it was reported that the relative densities of sample sintered at 1300°C for 1 h in air depend on the crystal structure of rare-earth oxides [14]. That is, for Sm_2O_3 and Eu_2O_3 (B-rare structure), the relative density was above 90%, however for Y_2O_3 and Er_2O_3 (C-rare structure), the relative density was as low as 75 to 80%. Since the crystal structure of rare-earth is

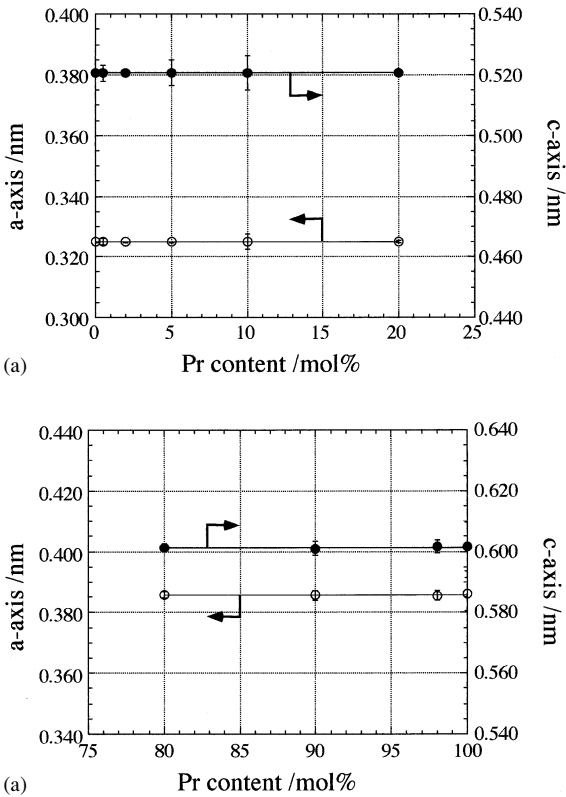


Fig. 2. (a) Change of lattice parameters of ZnO with Pr content after sintered at 1400°C in air followed by quenching into liquid nitrogen. (b) Change of lattice parameters of Pr₂O₃ with Pr content after sintered at 1400°C in air followed by quenching into liquid nitrogen.

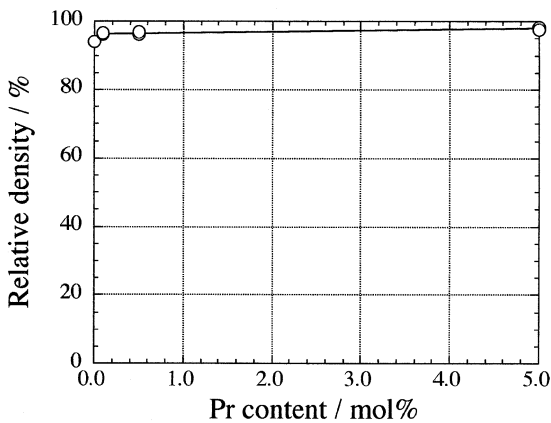


Fig. 3. Relationship between relative density and Pr content after sintered at 1350°C for 2 h in air.

prescribed by the ionic radii [15], these results suggest that the relative density of ZnO was improved by the addition of rare-earth element having larger ionic radii such as La and Pr. Though the experimental condition of our work was different from that in ref. 14, the tendency that higher relative density can be obtained was well agreed in the Pr₂O₃ doped ZnO.

Figure 4 shows change of the average grain size at the surface and the inside part of the pellets sintered at 1350°C for 2 h in air with Pr content [8]. “Inside part” means that region where the distance from the as-sintered surface was about 1800 μm (thickness of as-sintered pellet was about 3600 μm). This figure indicates that small amount of Pr about 0.1 mol% enhanced the average grain size, however, further addition of Pr more than 0.1 mol% brought about the decrease of the average grain size. The increase of average grain size by addition of small amount of dopant may be caused by the some kinds of lattice defect as reported in the La doped BaTiO₃ [16]. Further addition of Pr brought about the suppression of grain growth. The average grain size of the pellets which contained more than 10 mol% Pr was smaller than that of pure ZnO. Such suppression has been also reported for 2 mol% rare-earth (Sm, Eu, Y and Er) doped ZnO [14]. The reason of the suppression was considered to be pinning effect of the movement of grain boundary [17, 18]. Figure 4 also shows that no significant difference of average grain size was observed at the surface and in the inner part of the pellets. Figure 5 shows changes of grain size

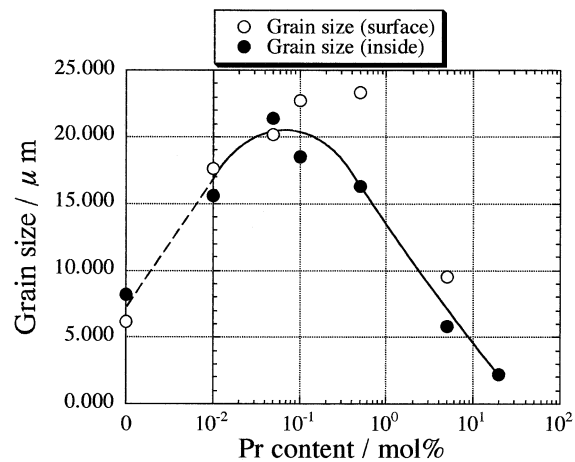


Fig. 4. Change of average grain size at the surface and inside part (around 1800 μm from the surface) of the pellets sintered at 1350°C for 2 h in air with Pr content [8].

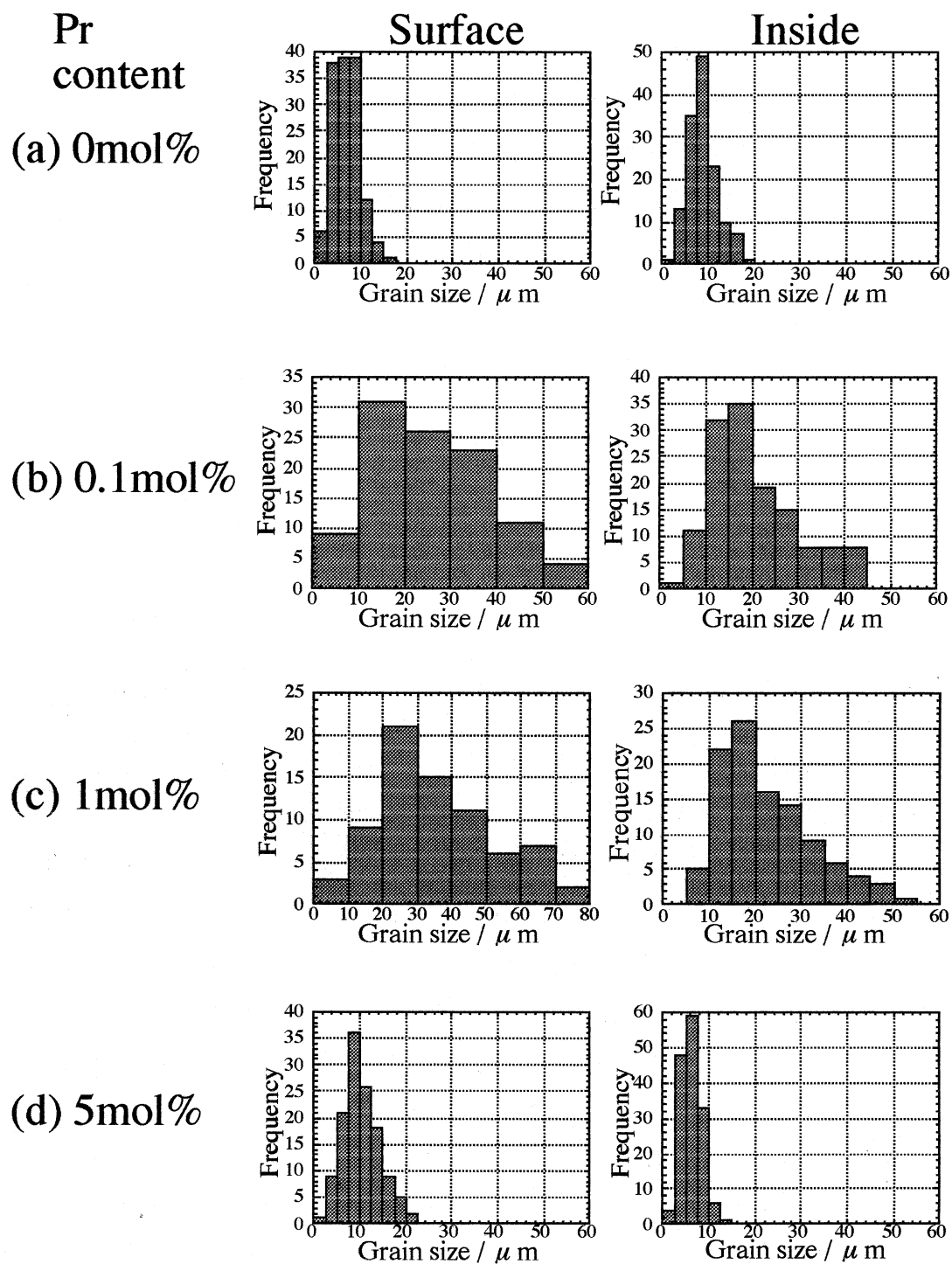


Fig. 5. Grain size distribution of Pr doped ZnO pellets at the surface and inside part of the pellets after sintered at 1350°C for 2 h in air. Pr content is (a) 0, (b) 0.1, (c) 1 and (d) 5 mol %, respectively.

distribution at the surface and inside part of the pellets sintered at 1350°C for 2 h in air as a function of Pr content. This figure indicates that the grain size distribution at the surface was wider than that inside part. During sintering, 0.6 wt % of weight loss was observed, that is, the Pr content at the surface could have concentration inhomogeneity, which may be brought about the wide grain size distribution at the surface. Figure 6 shows the comparison of grain size distribution of pellets (Pr content: 0.5 mol %) sintered at 1350°C for 2 h in air and that sintered at 1370°C for 1 h in air. As the sintering temperature increased up to 1370°C (just below the eutectic temperature), the tendency that wide grain size distribution can be observed at the surface was enhanced and abnormal grain growth was detected.

3.2. Change of Microstructure Below and Above Eutectic Temperature

Fig. 7 shows scanning electron micrographs of surface and inside parts of the pellets of 0.5 mol % Pr doped ZnO ceramics after sintered for 2 h in air at (a) 1300,

(b) 1400 and (c) 1500°C [8]. This figure shows that formation of “continuous distribution of the intergranular layer materials” [6, 19] was not observed at the surface of the pellet sintered at 1300°C but was clearly observed at 1400 and 1500°C. This result is in good agreement with the fact that the eutectic liquid phase forms at $1382 \pm 5^\circ\text{C}$. It has been reported that the component of the grain boundary phase is Pr_2O_3 and Pr_6O_{11} [6, 19, 20]. To clarify the distribution of the grain boundary phase, the depth profile of Pr content was measured. Figure 8 shows the depth profile of Pr content for the pellets sintered at 1350 and 1500°C for 2 h in air. For this experiment, samples having 0.5 mol % Pr doped ZnO were used. The weight loss after sintering was 0.6 % at 1350°C and 8.1 % at 1500°C [9]. For the pellet sintered in air at 1350°C (below eutectic temperature), it was clarified that the Pr content is almost constant from the surface into the bulk. On the other hand, for the pellet sintered in air at 1500°C (above eutectic temperature), Pr content at the surface is more than that inside part, and it gradually decreased with the distance from the surface. This implies that the formation of liquid

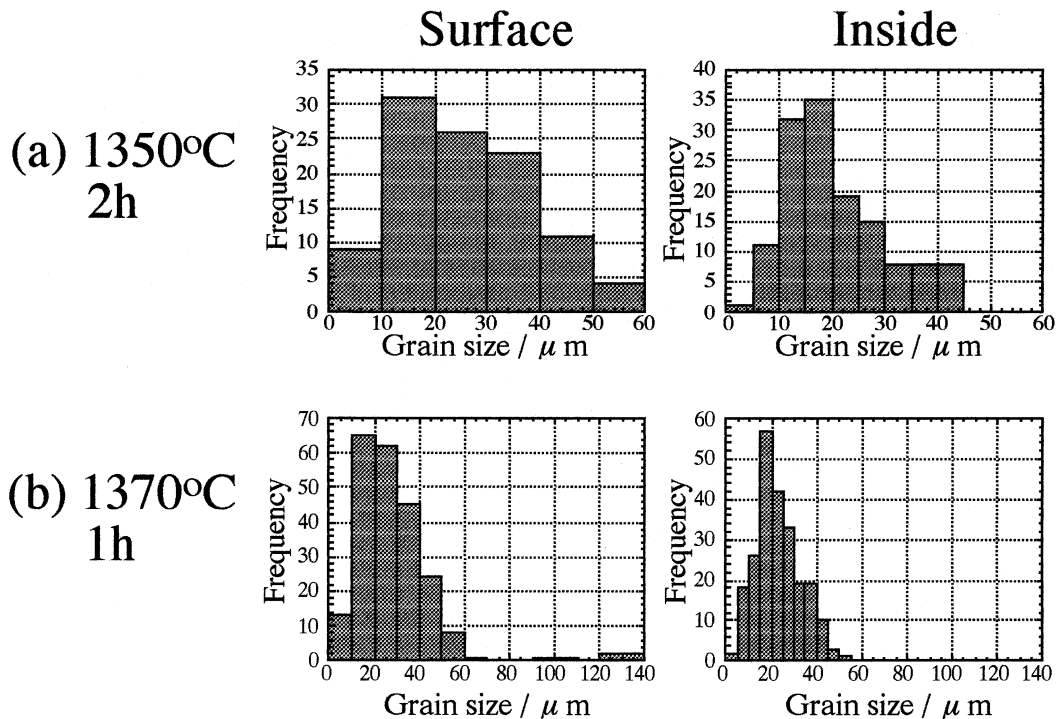


Fig. 6. Change of grain size distribution of 0.1 mol % Pr doped ZnO pellets at the surface and inside part of the pellets after sintered in air. (a) 1350°C for 2 h and (b) 1370°C for 1 h.

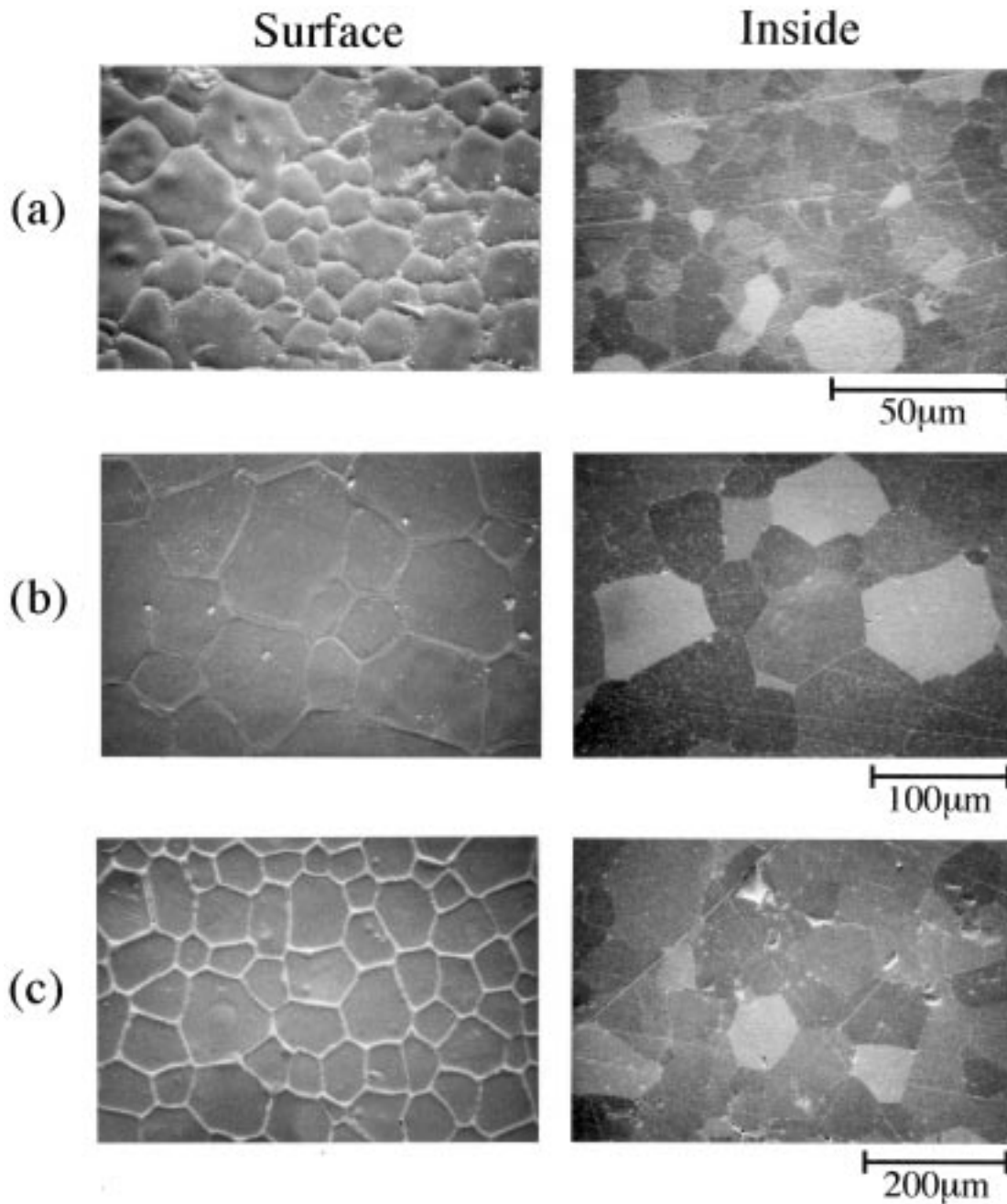


Fig. 7. Scanning electron micrographs of the surface and inside part of the pellets of 0.5 mol% Pr doped ZnO after sintered for 2 h in air at (a) 1300, (b) 1400 and (c) 1500°C [8].

phase caused the profile. In our previous work [9], the depth profile was measured for sample sintered in N_2 and O_2 . As the results, it was clarified that at 1350°C, no concentration gradient from the surface into the bulk was observed for pellets sintered for 2 h in both

N_2 and O_2 except that slight large Pr content was observed at the only surface region (0 to 50 µm) in N_2 . It was also clarified that at 1500°C, Pr concentration is considerably large at the surface of the pellets sintered for 2 h in N_2 , on the contrary, Pr content at the surface

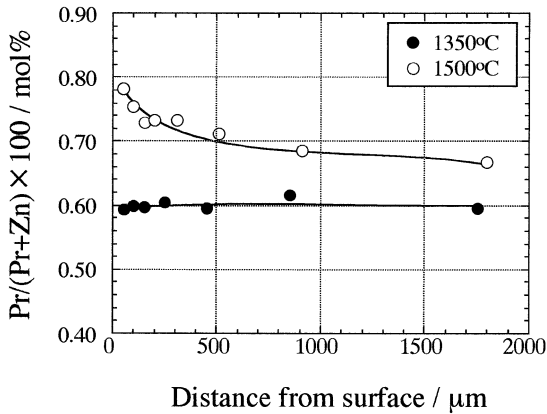


Fig. 8. Depth profile of Pr content for the pellet of 0.5 mol% Pr doped ZnO after sintered at 1350 and 1500°C for 2 h in air.

of the pellets sintered for 2 h in O_2 was small. The cause of the change of the Pr content with the sintering atmosphere was mainly attributed to the difference of the evaporated element. That is, it was concluded that Pr is preferentially evaporates in O_2 but Zn (is preferentially evaporates) in N_2 . These facts suggest that effect of preferential vaporization on composition change was small at 1350°C, on the other hand, ZnO tends to vaporizes preferentially from the surface at 1500°C. Figure 9 shows the depth profile of grain size for the pellet of 0.5 mol% Pr doped ZnO after sintered at 1350 and 1500°C for 2 h in air. This figure shows that grain size at the surface is slight larger than that inside part at both 1350 and 1500°C. In addition, suppression of grain growth was observed in the region between 50 and 300 μm from the surface

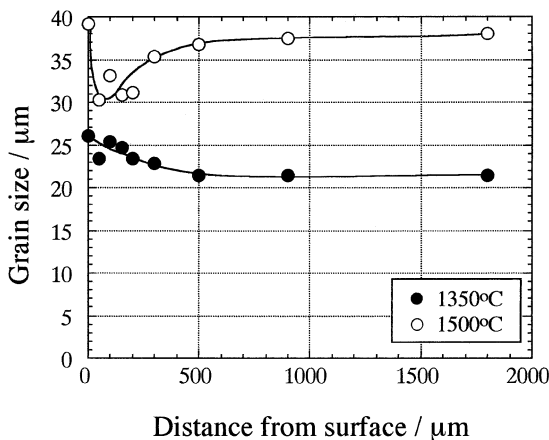


Fig. 9. Depth profile of grain size for the pellet of 0.5 mol% Pr doped ZnO after sintered at 1350 and 1500°C for 2 h in air.

at 1500°C. Comparing Fig. 8 and 9, the reason of the suppression of grain growth can be ascribed to the effect of pinning mentioned in Fig. 4 by the condensation of Pr due to the preferential vaporization of ZnO. Figure 10 shows the change of the grain growth rate and weight loss rate with sintering temperature in air [8]. This figure indicates that both grain growth rate and weight loss rate were drastically increased between 1350 and 1400°C. Since the liquid phase formation temperature is $1382 \pm 5^\circ\text{C}$, these drastic changes are believed to be ascribed to the formation of the liquid phase. Consequently, it can be considered that microstructure of Pr doped ZnO was determined by the mutual effect of liquid phase formation and vaporization of the components.

4. Conclusions

The effects of liquid phase and vaporization on the formation of the microstructure of Pr doped ZnO ceramics were discussed on the basis of the summary of our previous reports and our recent data, especially in air. In the ZnO- Pr_2O_3 binary system, eutectic liquid forms at $1382 \pm 5^\circ\text{C}$ and significant vaporization of the components occurred above the eutectic temperature. Entire achievement of this work was schematically shown in Fig. 11. Below eutectic temperature (1350°C), only 0.1mol% of Pr doping into ZnO brought about the grain growth of ZnO,

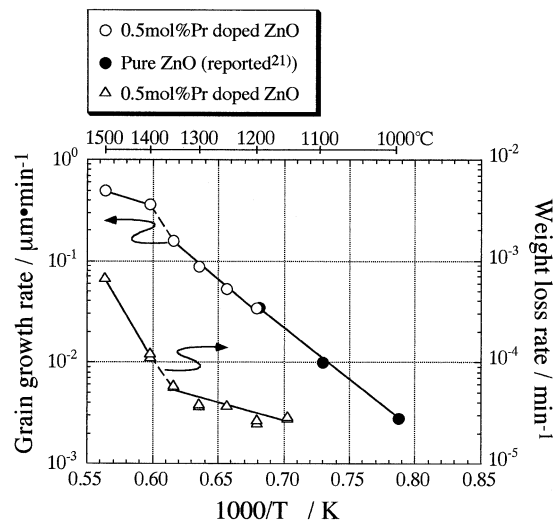


Fig. 10. Change of grain growth rate and weight loss rate with sintering temperature in air [8].

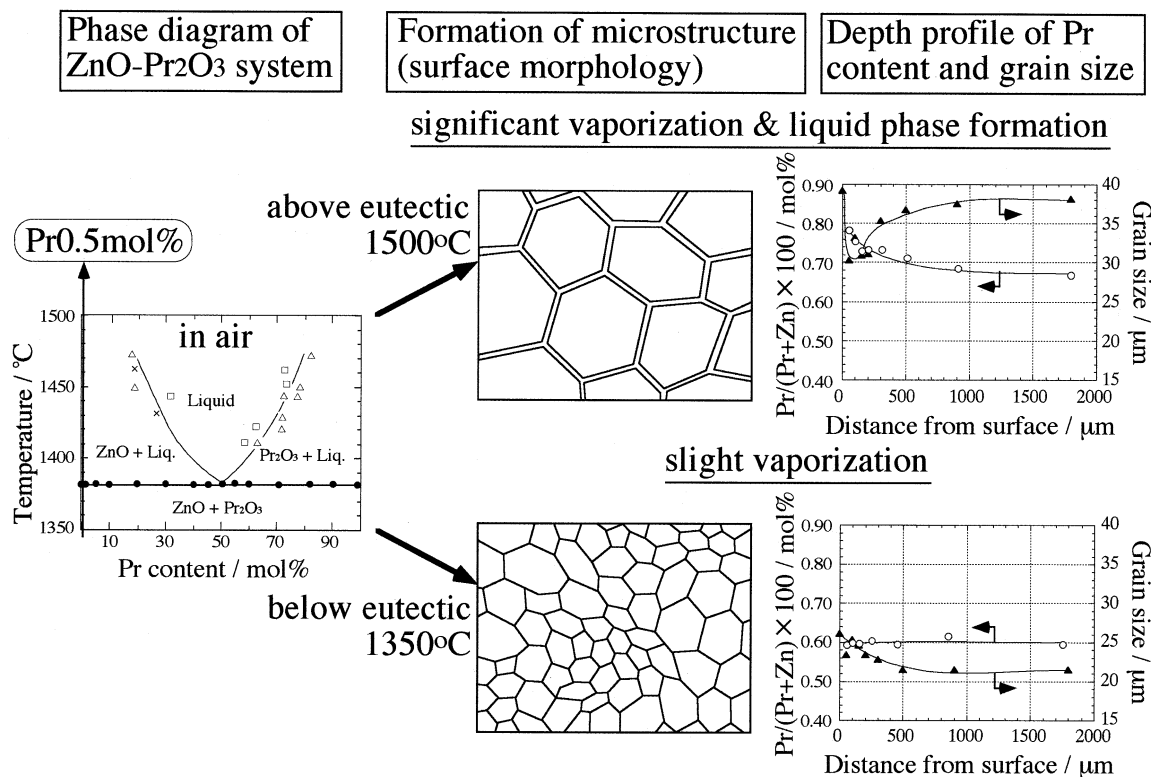


Fig. 11. Schematic drawing of entire achievement of this work.

however further addition of Pr brought about the suppression of the grain growth. Comparing the grain size distribution at the surface and the inside part of Pr doped ZnO ceramics, it was clarified that wider grain size distribution was observed at the surface. At the temperature just below the eutectic (1370°C), as well as the wide grain size distribution, abnormal grain growth was also observed. Above eutectic temperature, “continuous grain boundary phase” was clearly observed at the surface sintered in air. The depth profile of Pr content indicated that formation of concentration gradient was not observed below eutectic but above eutectic, relatively higher Pr content was observed at the surface. Formation of solid solution between ZnO and Pr₂O₃ was not observed or the solubilities were very small at both below and above eutectic temperature. Above the eutectic temperature, both grain growth rate and weight loss rate drastically increased between 1350 and 1370°C. It was clarified that the microstructure of Pr doped ZnO ceramics was determined by both

effects on the formation of liquid phase and on the vaporization of the components.

Acknowledgment

This work was supported by special coordination fund ‘Frontier Ceramics’ from Science and Technology Agency of Japan and Research Foundation for Material Science.

References

1. T. Masuyama, M. Matsuoka, and Y. Ida, *National Technical Report*, **15**, 216 (1968).
2. M. Namba, I. Nagasawa, M. Miyagawa, T. Ishii, K. Mukae, and K. Tsuda, *Fujijihou*, **47**, 1 (1974).
3. M. Matsuoka, *Jpn. J. Appl. Phys.*, **10**, 736 (1971).
4. J. H. Hwang, T. O. Mason, and V. P. Dravid, *J. Am. Ceram. Soc.*, **77**, 1499 (1994).
5. G. Y. Sung, S. McKernan, and C. B. Carter, *J. Mater. Res.*, **7**, 474 (1992).

6. A. B. Alles and V. L. Burdick, *J. Appl. Phys.*, **70**, 6883 (1991).
7. A. B. Alles, R. Puskas, G. Callahan, and V. L. Burdick, *J. Am. Ceram. Soc.*, **76**, 2098 (1993).
8. M. Shida, S. Y. Chun, N. Wakiya, K. Shinozaki, and N. Mizutani, *J. Ceram. Soc. Jpn.*, **104**, 44 (1996).
9. S.-Y. Chun, N. Wakiya, K. Shinozaki, and N. Mizutani, *J. Ceram. Soc. Jpn.*, **104**, 1056 (1996).
10. S.-Y. Chun, N. Wakiya, H. Funakubo, K. Shinozaki, and N. Mizutani, *J. Am. Ceram. Soc.*, **80**, 995 (1997).
11. T. Sakurai, *Universal Program System for Crystallographic Computation* (Crystallographic Society of Japan, 1967).
12. R. L. Fullman, *J. Met.*, **5**, 447 (1953).
13. I. S. Kulikov, *Thermodynamika Okidov Spravochnik* Nisso Tsuushinsha, Moscow, USSR, 1986) p. 263
14. K. Hamano, S. Ri, and Z. Nakagawa, *Yogyo-Kyokai-Shi*, **92**, 46 (1984).
15. F. S. Galasso, *Structure and Properties of Inorganic Solids*, (Pergamon Press Inc., 1970) p. 99
16. M. Drofenik, *J. Am. Ceram. Soc.*, **5**, 311 (1987).
17. P. J. Jorgensen and P. C. Andersen, *J. Am. Ceram. Soc.*, **48**, 207 (1965).
18. W. D. Kingery, H. K. Bowen, and D. R. Uhlmann, *Introduction to ceramics*, 2nd ed, pp. 171–448 (Wiley, New York, 1976).
19. Y. S. Lee, K. S. Liao, and T. Y. Tseng, *J. Am. Ceram. Soc.*, **79**, 2379 (1996).
20. I. G. Solorzano, J. B. V. Sande, K. K. Baek, and H. L. Tuller, *Mat. Res. Soc. Symp. Proc.*, **295**, 189 (1993).
21. S. K. Dutta and R. M. Spiggs, *J. Am. Ceram. Soc.*, **53**, 61 (1970).